

CARTOGRAPHIC STUDY OF THE MEO PHASE SPACE FOR PASSIVE DEBRIS REMOVAL

D. K. Skoulidou, A. J. Rosengren, K. Tsiganis, and G. Voyatzis

*Department of Physics, Aristotle University of Thessaloniki, 54124 Thessaloniki, Greece,
Email: dskoulid@physics.auth.gr, aaronjay@physics.auth.gr, tsiganis@auth.gr, voyatzis@auth.gr*

ABSTRACT

Space debris mitigation is one of the most important problems of space science and applications. In this work, we present our recent investigations on the possibility of exploiting the natural long-term dynamics of artificial satellites and debris to address the problem of designing passive mitigation strategies. Our work consists of the characterization of regular and chaotic, long-term stable and unstable, dynamical behaviors in the circumterrestrial phase space and, in particular in the Medium-Earth Orbit (MEO) phase space region, with particular focus in the orbital region of GNSS and the GTOs. Using a suitably modified version of the SWIFT symplectic integration package that has been extensively used in the past for asteroid dynamics, we construct a numerical cartography of dynamical lifetimes and eccentricity variation in the MEO phase-space.

Keywords: space debris mitigation, passive migration strategies, satellites: dynamical evolution and stability.

1. INTRODUCTION

Recently, it has been realized that luni-solar secular resonances are of particular importance in the Medium Earth Orbit (MEO) region, as they may provide a substantial perigee boost for a satellite, under properly chosen orbital circumstances [9, 3, 2, 4]. Additionally, solar radiation pressure (SRP) can play a crucial role in the motion of satellites, especially at large altitudes [1, 5].

Our goal is to understand the long-term behavior of circumterrestrial orbits and benefit from that in order to find natural re-entry paths for passive removal of inactive satellites and debris. For that purpose, we numerically integrated the trajectories of millions of initial conditions, using the full (i.e. non-averaged) equations of motion and a suitable dynamical model, covering the whole circumterrestrial region. After building a “low-resolution” map for the whole region, we focused in the orbital domains of (a) the Global Navigation Satellite Systems (GNSS) and (b) the Geostationary Transfer Orbits (GTO)s.

In section 2, we describe the dynamical model used and the choice initial conditions. A subset of our results is presented in section 3, followed by our conclusions in section 4.

2. PROBLEM FORMULATION

2.1. Model

A satellite orbiting around the Earth is affected mainly by the following perturbations: the Earth’s oblateness, the higher harmonics of the Earth’s geopotential, the lunar and solar gravitational fields, the direct solar radiation pressure and atmospheric drag. The latter particularly affects low-altitude orbits in the Low Earth Orbit (LEO) region.

In our study, we wish to understand the long-term dynamical behavior of satellite orbits, focusing mainly in the MEO (i.e. GNSS) and GTO part of the phase space. To that purpose, a gravitational model that includes the Earth’s gravity field up to degree and order 2 (i.e. $J_{2,0}$, $J_{2,2}$), the luni-solar gravitational potential and direct radiation pressure is adequate.

For the numerical integrations, we used a suitably modified version of the SWIFT symplectic integration package by Levison and Duncan [6]. SWIFT is well suited for dynamical studies of test particles, affected by a massive central body and perturbed by other massive bodies. The full equations of motion are used and solve by a symplectic scheme, which preserves the conservative form of the equations and leads to a small, bounded error in energy, even for very long times. SWIFT-SAT is also modified in order to account for the 2^{nd} degree and order geopotential. Special care has to be taken for the “perturbation” caused by the Sun, as it is more massive than the Earth and the traditional symplectic scheme could fail. For this reason we first solved for the motion of the Sun and the Moon in the full N -body problem of the solar system, thus creating a very precise ephemeris for these two bodies. SWIFT-SAT then reads in the positions of these perturbing orbits to compute their direct effect on a satellite. The effect of SRP on a satellite has also been added, using

Table 1. Grids of initial conditions for the LEO-to-GEO study, for dynamical maps in $a - e$ phase space.

| | ALL* | GTO† | MEO |
|-------------------------------------|-------------------|--|---------------|
| \mathbf{a} (\mathbf{a}_{GEO}) | 0.150 – 1.050 | 0.498 – 0.664 | 0.600 – 0.710 |
| Δa | 0.0050 | 0.00475 | 0.0025 |
| \mathbf{e} | 0 – 0.9 | 0.5 – 0.8 | 0 – 0.88 |
| Δe | 0.015 | 0.015 | 0.02 |
| \mathbf{i} ($^\circ$) | 0 – 120 | 0.235 – 10.235 23.533 – 33.533 41 – 51 | 0 – 90 |
| Δi ($^\circ$) | 2 | 1 | 2 |
| $\Delta\Omega$ ($^\circ$)† | {0, 90, 180, 270} | | |
| $\Delta\omega$ ($^\circ$)† | {0, 90, 180, 270} | | |
| # of orbits | ~ 8 m | ~ 1.6 m | ~ 6 m |

* Only three angle sets ((a) $\Delta\Omega = 0, \Delta\omega = 0$, (b) $\Delta\Omega = 180^\circ, \Delta\omega = 90^\circ$ and (c) $\Delta\Omega = 270^\circ, \Delta\omega = 90^\circ$) were used for the full LEO-to-GEO maps.

† The satellite’s initial node and perigee angles were referenced with respect to the equatorial lunar values at each epoch, excepting the GTO maps where the Moon’s ecliptic angles were used instead.

the standard cannonball approximation [8]. The units are chosen so that the gravitational constant is $\mathcal{G} = 1$ and the units of length and time are accordingly chose such that, following Kepler’s third law, the geosynchronous radius $a_{GEO} = 1$ (~ 42164.17 km) and the period of Earth’s rotation (1 sidereal day = 23h 56m 4.1s) are equal to unity.

2.2. Initial Conditions

Our goal is to obtain a global view of the long-term dynamics circumterrestrial orbits. For that purpose, we covered a wide range in orbital elements space and propagated the initial conditions over a long timescale (120 years).

A coarse grid of initial conditions was constructed to cover the whole area from LEO to GEO, while higher-resolution grids were constructed for the GTO and MEO areas, focusing on the GNSS region. The summary of our chosen initial conditions is shown in table 1. The initial mean anomaly was set equal to zero, $M = 0$, for all cases.

The study was repeated for two selected initial epochs, namely JD 2458475.2433 (22.74/12/2018) – $\lambda_{Sun} = 270.475^\circ$ – and JD 2459021.7800 (21.28/06/2020) – $\lambda_{Sun} = 90.086^\circ$ – hereafter designated simply as “2018” and “2020”, respectively. The timespan of all integrations was set to 120 yr. All simulations were carried out for a nominal value of the SRP coefficient, namely $C_r(A/m) = 0.015$ m²/kg, but also repeated for an “enhanced SRP” coefficient of 1 m²/kg; this was done in order to probe the different dynamics that a satellite would experience, if a SRP-augmenting device (e.g. a large solar sail) was on-board. In all cases, we set the limit for re-entry at an altitude of $h = 400$ km, since we did not include atmospheric drag.

3. RESULTS

3.1. Circumterrestrial phase space

In this section is presented a subset of the atlas of dynamical lifetime (i.e. time until re-entry) and maximum eccentricity attained (sup- e) maps for the circumterrestrial phase space. Figures 1 and 2 show the results corresponding to a given initial phase angle combination $\Delta\Omega = 270^\circ, \Delta\omega = 90^\circ$ and for different initial inclinations. The values of $i = 6^\circ$ and 46° , which are close to latitudes of the Kourou and Baikonur launching sites respectively, correspond to inclinations of possible GTOs launched from these sites. On the other hand, the values of 56° and 64° are close the nominal constellation inclinations for Galileo and GLONASS, respectively. Note that the gray curve appearing in all these figures is the curve of constant perigee altitude equal to 400 km, which defines, for every value of a , the critical eccentricity at which the orbit is considered as having re-entered in the atmosphere of the Earth.

For inclinations smaller than $\sim 40^\circ$ and for the nominal SRP value, the orbits are generally stable. For the enhanced SRP run, an instability hatch opens up at $a \sim 0.2$, along the re-entry corridor of the gray critical curve and continues down to lower eccentricities and semimajor axes. This re-entry route is due to a resonance due to SRP and oblateness [7, 1, 5], and its location shifts towards lower altitudes with increasing inclination. The maps for the high inclination regions exhibit more complicated and interesting features, because of the strong interactions due to luni-solar secular resonances. Generally, many disposal hatches appear near the operational satellites’ inclinations, depending though on the initial orientational angles – this is expected, as each luni-solar resonance can be stable (i.e. keeping the eccentricity small for long times) or unstable (i.e. leading to eccentricity growth),

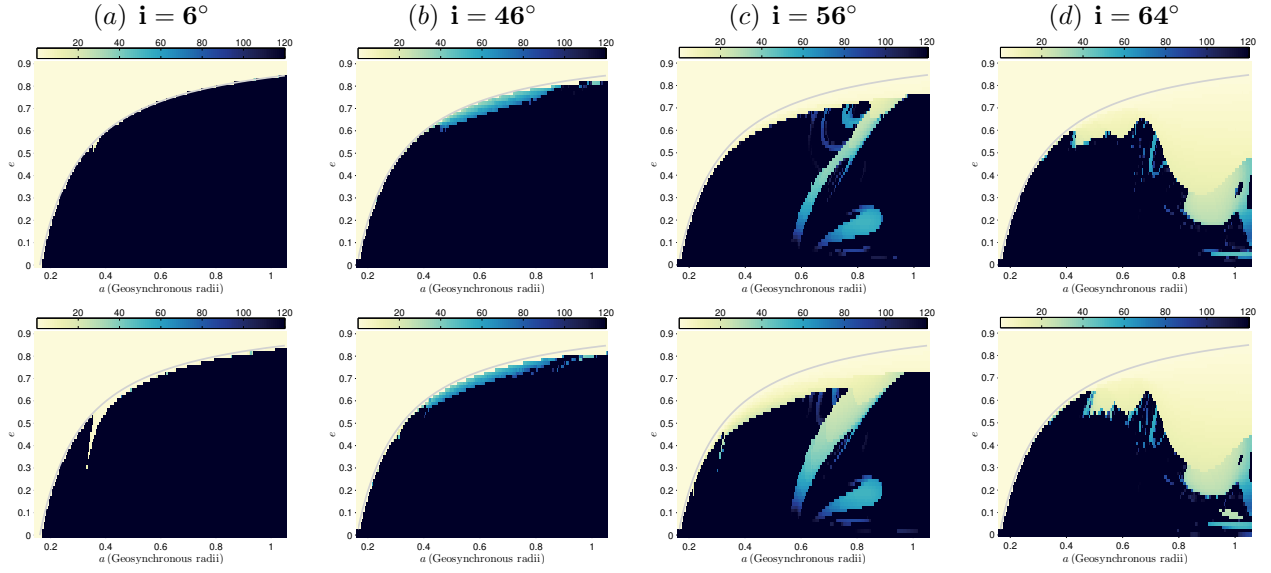


Figure 1. Lifetime of the global LEO-to-GEO phase space for various values i , $\Delta\Omega = 270^\circ$, $\Delta\omega = 90^\circ$, epoch 2018, and for two effective area-to-mass ratios (m^2/kg), 0.015 (top) and 1 (bottom). The colorbar for the lifetime maps is from 0 to 120 years.

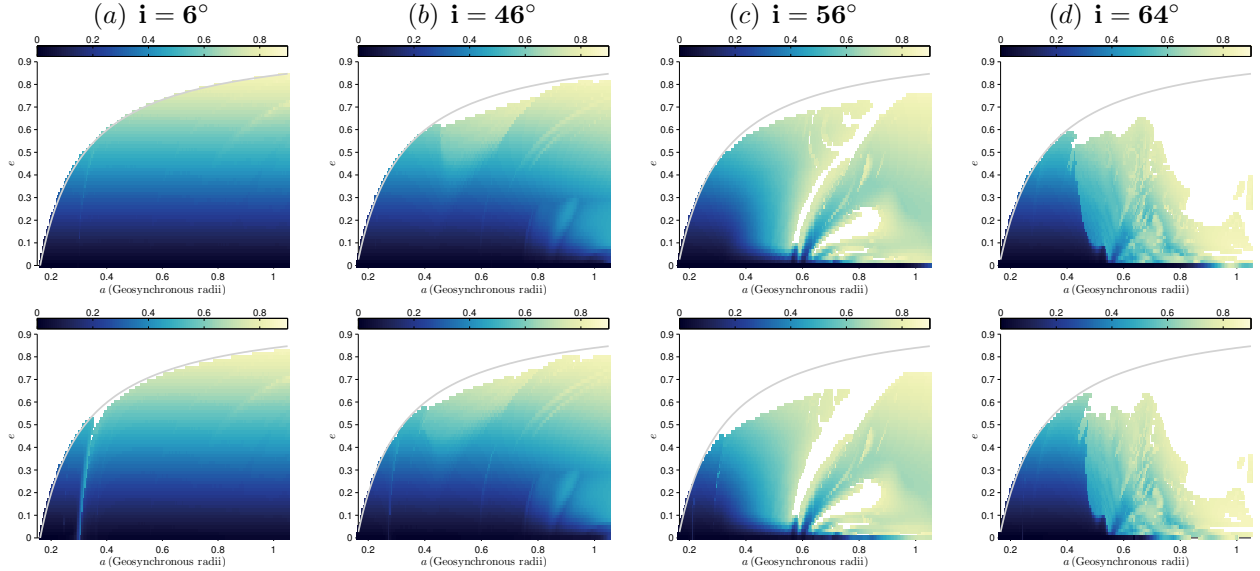


Figure 2. Sup- e maps of the global LEO-to-GEO phase space for various values i , $\Delta\Omega = 270^\circ$, $\Delta\omega = 90^\circ$, epoch 2018, and for two effective area-to-mass ratios (m^2/kg), 0.015 (top) and 1 (bottom). The colorbar for the sup- e maps is from eccentricity 0 to 0.85.

depending on whether the orbit departs near its stable or unstable fixed point in phase space. Our results also show that an enhanced SRP tends to expand these reentry corridors. In sections 3.2 and 3.3, the GNSS and GTO phase space regions are treated in more detail.

3.2. MEO phase space

The MEO orbits of the GNSS are affected strongly by the interplay between luni-solar resonant perturbations

and the effects caused by the Earth's predominant gravitational harmonic. The evolution of the perigee altitude is related to the eccentricity of an orbit and any large-amplitude variation in e , e.g. due to a resonance, can prolong or shorten the dynamical lifetime of a satellite.

In figures 3 and 4 we present the lifetime and sup- e stability maps for initial inclinations equal to 56° and 64° , i.e. near the Galileo and GLONASS nominal constellation inclinations, respectively. The maps were derived for two different phase angles combinations, namely $\Delta\Omega = 90^\circ$, $\Delta\omega = 180^\circ$ and $\Delta\Omega = 270^\circ$, $\Delta\omega = 90^\circ$.

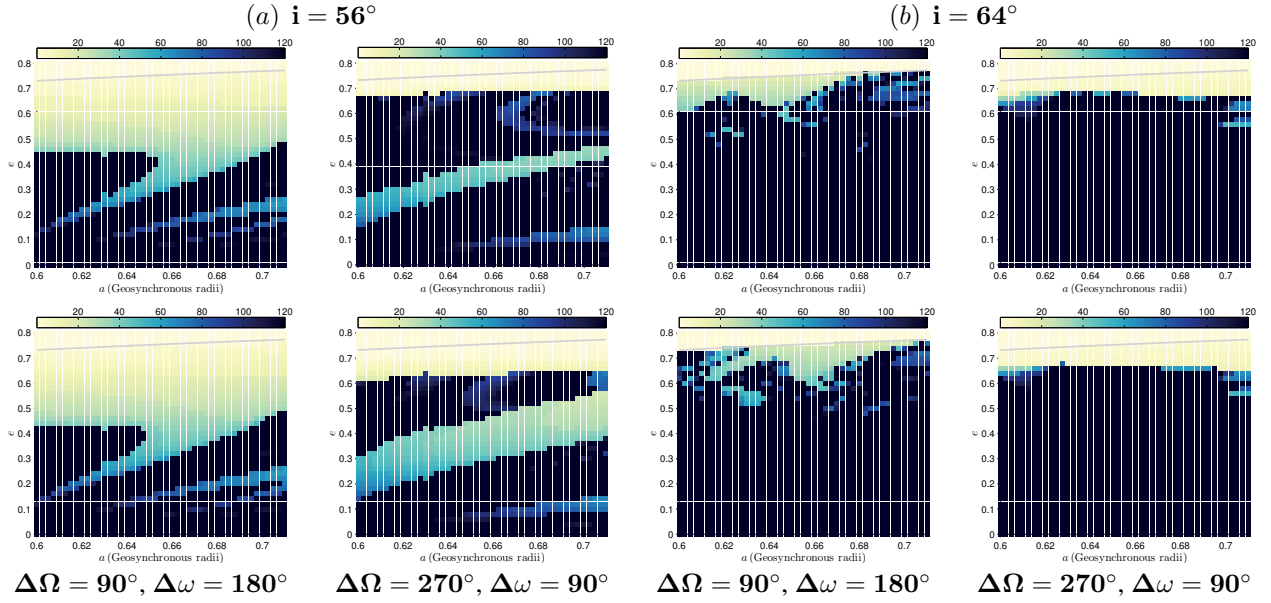


Figure 3. Lifetime of the global MEO phase space for: (a) $i = 56^\circ$ and epoch 2018, (b) $i = 64^\circ$ and epoch 2020, $\Delta\Omega = 90^\circ$, $\Delta\omega = 180^\circ$ (left) and $\Delta\Omega = 270^\circ$, $\Delta\omega = 90^\circ$ (right), and for two effective area-to-mass ratios (m^2/kg), 0.015 (top) and 1 (bottom). The colorbar for the lifetime maps is from 0 to 120 years.

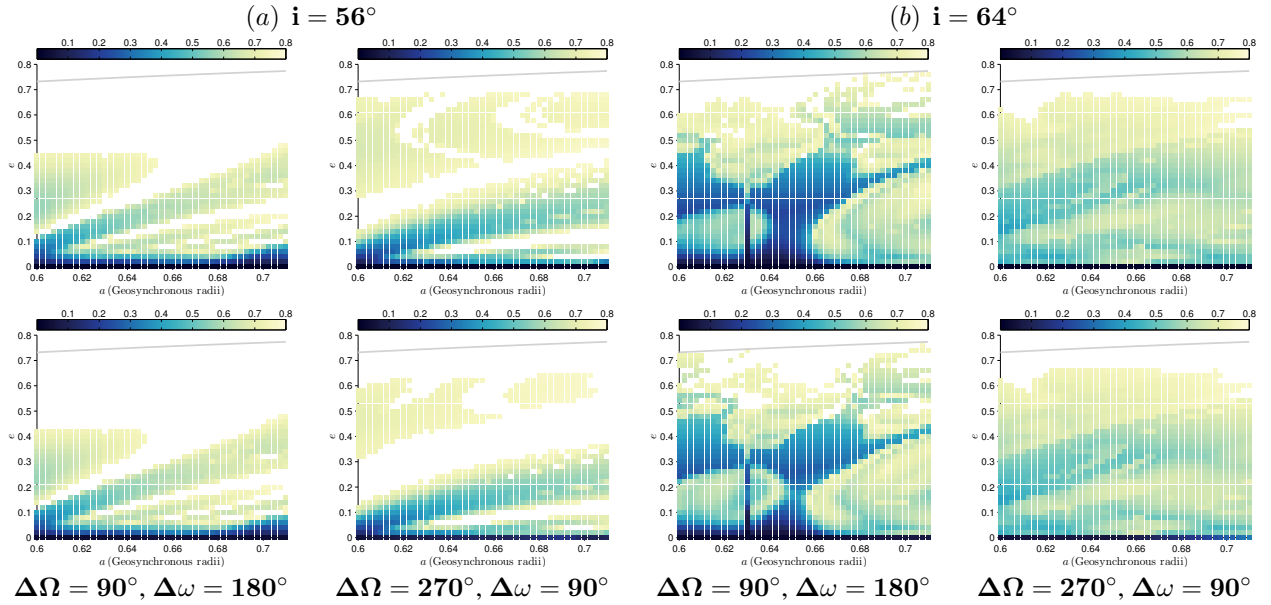


Figure 4. Sup- e maps of the global MEO phase space for: (a) $i = 56^\circ$ and epoch 2018, (b) $i = 64^\circ$ and epoch 2020, $\Delta\Omega = 90^\circ$, $\Delta\omega = 180^\circ$ (left) and $\Delta\Omega = 270^\circ$, $\Delta\omega = 90^\circ$ (right), and for two effective area-to-mass ratios (m^2/kg), 0.015 (top) and 1 (bottom). The colorbar for the sup- e maps is from eccentricity 0 to 0.8.

The long-term effect of luni-solar resonances depends strongly on the choice the initial orientational angles. For GPS and Galileo inclinations, many interesting disposal hatches occur at moderate and low eccentricity phase space, leading to lifetimes of order 40 – 60 yr , for eccentricities smaller than 0.15. For the GLONASS inclination band, the disposal regions generally occur at higher eccentricities, which would make it harder to actually use for passive re-entry. At all constellation inclinations, an augmented SRP slightly widens these re-entry regions,

but without deforming them considerably.

3.3. GTO phase space

GTOs are mostly concentrated around $a \approx 0.6 \cdot a_{GEO}$, with eccentricities around 0.6. They are grouped in inclinations bands, which related to the main launch sites of Kourou, KSFC and Baikonur. In figures 5 and 6 the

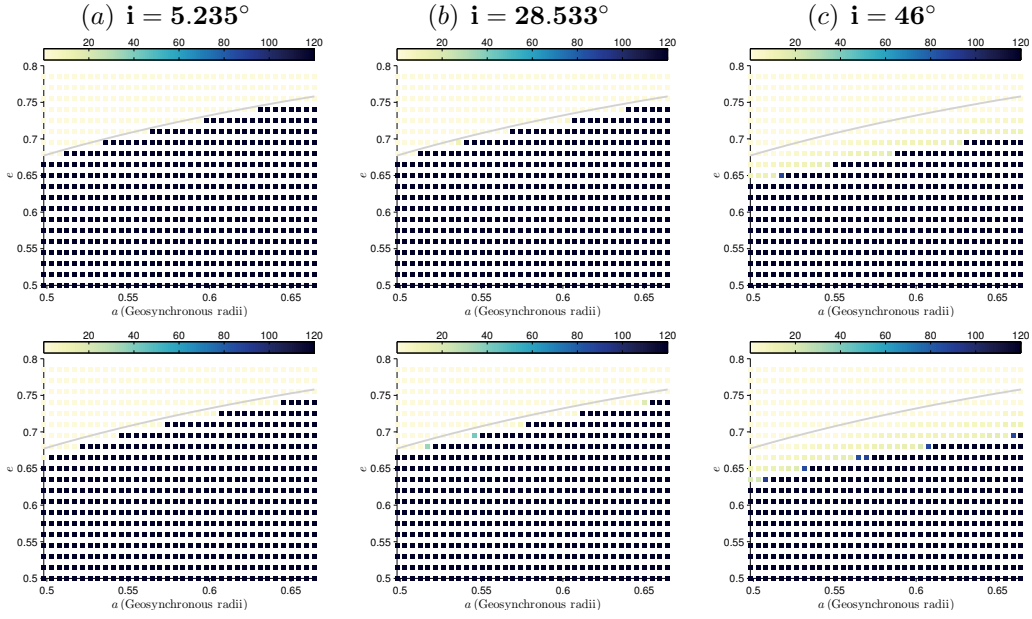


Figure 5. Lifetime of the global GTO phase space for latitudes near Kourou (left), Cape Carneval (middle), and Baikonur (right), $\Delta\Omega = 90^\circ$, $\Delta\omega = 0$, epoch 2018, and for two effective area-to-mass ratios (m^2/kg), 0.015 (top) and 1 (bottom). The colorbar for the lifetime maps is from 0 to 120 years.

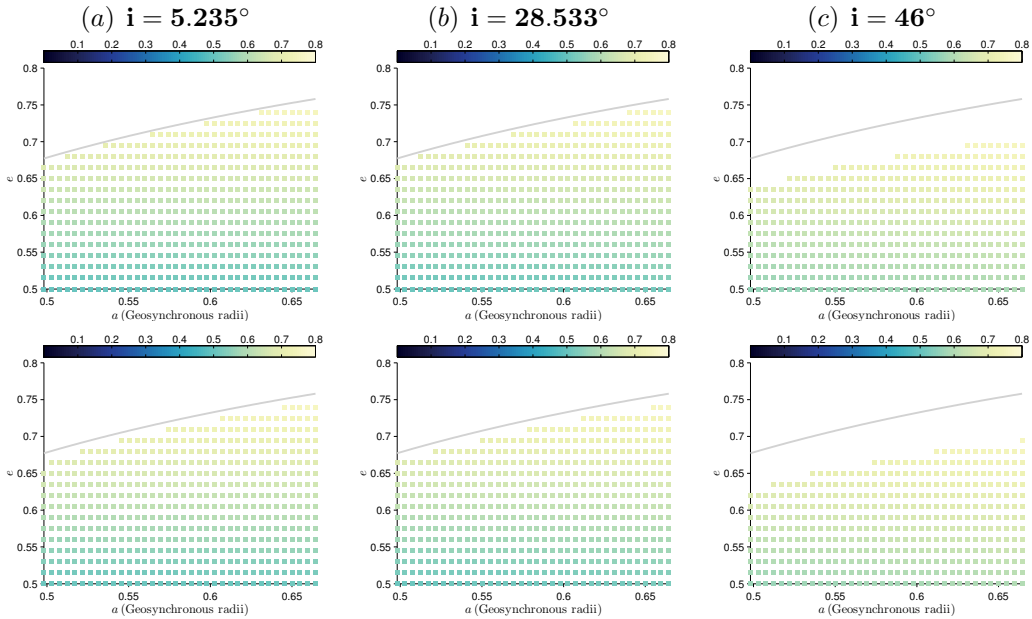


Figure 6. Sup- e maps of the global GTO phase space for latitudes near Kourou (left), Cape Carneval (middle), and Baikonur (right), $\Delta\Omega = 90^\circ$, $\Delta\omega = 0$, epoch 2018, and for two effective area-to-mass ratios (m^2/kg), 0.015 (top) and 1 (bottom). The colorbar for the sup- e maps is from eccentricity 0 to 0.8.

lifetime and sup- e stability maps are presented, for inclinations equal to 5.235° , 28.533° and 46° and for an initial orientation given by $\Delta\Omega = 90^\circ$, $\Delta\omega = 0$.

The results show that, at low to moderate inclinations, long-term orbital deformations are not very important, in the sense that very few orbits, started already very close to the critical eccentricity line, manage to re-enter naturally. Adding atmospheric drag in our model might help,

although the altitude is quite high – this is under investigation. For highly-inclined orbits, natural re-entry appears to be easier for GTOs with $e \sim 0.6$, since the lifetimes are shorter than 120 years for a wider region. Artificial enhancement of SRP could further expand the re-entry regions, although not very much.

4. CONCLUSIONS

The purpose of our study is to understand the long-term dynamical evolution of Earth satellite orbits in the usable circumterrestrial space and to find natural ‘highways’, suitable for passive debris mitigation (natural re-entry). We focused mostly in the GNSS and GTO regions, which are two of the most interesting regions for satellite use. We numerically integrated the trajectories of millions of initial conditions, using a suitable dynamical model that takes into account the most important effects acting in this orbital region, and repeated the computations both for the nominal and for an “enhanced-SRP” problem.

In the GNSS region, the effects of luni-solar resonances depend strongly on the choice of initial orientational angles. Many interesting disposal hatches occur at moderate to low eccentricities, for the inclination values of the real GNSS. SRP does not change dramatically these phase-space structures, but widens the escape hatches. Lifetimes of order 40 – 60 *yr* are feasible, for eccentricities smaller than 0.15. A preliminary analysis suggests that these lifetimes can be achieved by performing a relatively costly but still reasonable impulsive maneuver, with ΔV of order 10%. In this way a low-eccentricity operational satellite can be forced to “jump” on a disposal orbit that will lead to re-entry after a reasonable amount of time. Note that a re-entry time of 40-60 years for a MEO satellite does not violate the IADC rules for the protected LEO region, as most of the time is spent far away from LEO altitudes and the satellite would only make brief passages through the protected LEO area, with the cumulative time spent on this region being much less than 25 years. A complete analysis of requirements for reaching the optimal re-entry solution for each MEO orbit is among the goals of our project and is currently under way.

For the GTO region, at low and moderate inclinations (i.e. Kourou and KSFC), long-term orbital instabilities are not observed, at least for the majority of our (nominal SRP) cases. For highly-inclined orbits, re-entry is easier for orbits with initial $e \sim 0.6$ and an enhanced SRP does expand the re-entry regions, but not very much. Hence, GTOs appear to be among the hardest cases in MEO, in terms of finding a natural highway to re-entry. The results might improve if we take into account the weak effects of atmospheric drag, in particular if we consider and enhanced area-to-mass ratio (i.e. a “drag” sail, in place of a SRP-sail). This matter is currently under investigation. We have to check that case.

ACKNOWLEDGMENTS

This research is funded by the European Commissions Horizon 2020, Grant Agreement 687500 (project ReD-SHIFT). <http://redshift-h2020.eu/>

REFERENCES

1. Colombo C., Lucking C., McInnes C. R., (2012). Orbital dynamics of high area-to-mass ratio spacecraft with J_2 and solar radiation pressure for novel Earth observation and communication services, *Acta Astronautica*, **81**, 137–150”
2. Celletti A., Galeş C., Pucacco G., (2016). Bifurcation of lunisolar secular resonances for space debris orbits, *SIAM Journal on Applied Dynamical Systems*, **15**, 1352–1383
3. Daquin J., Rosengren A. J., Alessi E. M., Deleflie F., Valsecchi G. B., Rossi A., (2016). The dynamical structure of the MEO region: long-term stability, chaos, and transport, *Celestial Mechanics and Dynamical Astronomy*, **124**, 335–366
4. Gkolias I., Daquin J., Gachet F., and Rosengren A. J., (2016). From order to chaos in Earth satellite orbits, *The Astronomical Journal*, **152**, 119 (15pp)
5. Lantukh D., Russell R. P., Broschart S., (2015). Heliotropic orbits at oblate asteroids: balancing solar radiation pressure and J_2 perturbations”, *Celestial Mechanics and Dynamical Astronomy*, **121**, 171–190
6. Levison H., Duncan M., (1994). The long-term dynamical behavior of short-period comets, *Icarus*, **108**, 18–36
7. Hamilton D. P., Krivov A. V., (1996). Circumplanetary dust dynamics: effects of solar gravity, radiation pressure, planetary oblateness, and electromagnetism, *Icarus*, **123**, 503–523
8. McInnes C. R., (1999). *Solar Sailing: Technology, Dynamics and Mission Applications*, Springer-Verlag
9. Rosengren A. J., Alessi E. M., Rossi A., and Valsecchi G. B., (2015). Chaos in navigation satellite orbits caused by the perturbed motion of the Moon *MNRAS*, **449**, 3522–3526